

Compact-Size Fractal Antenna with Stable Radiation Properties for Wi-Fi and WiMAX Communications

Amer T. Abed^{1,2}, Mandeep S. J. Singh¹ and Mohammad T. Islam¹

¹ Department of Electrical, Electronic and Systems Engineering
Universiti Kebangsaan Malaysia (UKM),
Selangor, Malaysia.

² AL-MAMON University College
14th Ramadhan street, Baghdad, Iraq
[E-mail : amer.t.abed@ieee.org]

*Corresponding author: Amer T. Abed

*Received October 13, 2017; revised January 3, 2018; accepted January 30, 2018;
published June 30, 2018*

Abstract

In this study, a novel fractal ring antenna with a compact size of $24 \times 9 \times 0.8 \text{ mm}^3$ was configured using three iterations. Low profile, circular polarization, and measured operating bands (4.5–6.5 GHz) meet specifications of the upper band used in Wi-Fi and WiMAX applications. The antenna featured, stable radiation properties, especially gain and efficiency, in the notched band (92%). In deep, the antenna impedance, reflection coefficients, surface current distribution and circular polarization for the three iterations had been studied to improve the process of antenna design and its radiation characteristics

Keywords: Fractal ring, compact size, Wi-Fi and WiMAX

1. Introduction

By the invention of radio, a revolution of communication began, which elevated to a new level by the introduction of modern technologies such as satellite, cell phone, GPS, W-Fi and WiMAX. With these modern technologies, voice, data and multimedia transceived between users at anytime and anywhere with very high speed and capacity. The increasing use of the number of wireless communication equipment, especially the portable types, has provided competitive opportunities in the market to meet the needs. One of the most important parts of these communication devices is the antenna, so many types of antennas had been designed to fulfill the stringent requirement of the modern communication systems. Given the increasing use of wireless local area network (WLAN) and Worldwide Interoperability for Microwave Access (WiMAX) in recent years [1,2], different antennas for WLAN/wireless fidelity (Wi-Fi) standards of 2.4–2.484/5.15–5.825 GHz and WiMAX standards of 2.5–2.6/3.4–3.6/5.25–5.85 GHz has been designed to support these types of wireless communication.

When the length of the antenna is less than quarter of the wavelength of the operating frequency, it is difficult to have good radiation properties. But through using a fractal geometry antenna, where the shape is repeated in a limited size, in a way that increases the total length of the antenna to match, for example, half of the wavelength of the corresponding desired frequency, the size limitations can be overcome in this case. There many fractal geometries such as the tree, Koch, Minkowski and Hilbert fractals that are used in designing this type of antenna [3].

Universal serial bus (USB) dongles are used in many portable communication devices, such as laptops and PADS, to transmit and receive data with high bit rate. Although USB dongles used with portable devices, the desired antenna must solve serious challenges, such as size, multi band, and stability of radiation characteristics (gain and efficiency) in notched bands.

2. Related Work

Recently, researchers attempted to apply certain monopole antennas of different shapes such as: loop spiral [4], planar monopole [5], ground slotted [6], monopole fed by CPW [7], strip-monopole [8], as USB dongles. A compact UWB antenna was presented in [9], a loading loop resonator was used in this design to achieve notched bands of 5.2-5.7 GHz. Interferences of 3.5 GHz are rejected by folding the arms of the fork-shaped radiator. The physical size of the antenna is 30 mm × 21 mm × 0.8 mm, a gear-shaped tooth structure fed by a small CPW was used in the design of the antenna in [10], the notched band is 2.39-24.53 GHz with LP. The compact size of the antenna is 30 mm × 30 mm × 1.6 mm. Three conductive layers in the structure of the mushroom metamaterial used in the substrate-integrated waveguide cavity-backed slot antenna in [11] has a complex structure and covers only the upper band used for Wi-Fi and WiMAX applications. The frequency range (1.5-4)GHz with LP radiation by using Koch snowflake fractal shaped antenna reported in [12], the geometry of the fractal antenna is, the overall size of the antenna is 80x40x1.58 mm. [13] designed a Minkowski model fractal loop monopole antenna fabricated on an FR4 substrate with an overall size of 10 mm × 45 mm × 0.8 mm. The antenna was configured by three iterations to cover frequency bands of 2.3-3.9 and 4.9-5.4 GHz. [14] investigated an H-fractal antenna that

was configured by seven iterations. The antenna was fabricated on an FR4 dielectric substrate with dimensions of 120 mm × 120 mm × 1.6 mm to achieve dual operating bands 2.4-2.49 and 5.1-5.8 GHz. [15] Used Wunderlich-shaped fractal split ring resonator (WSRR) to create CP radiation in designing the proposed antenna to achieve ARBW 1.86% of the operating band 3.4-3.6 GHz. [16] reported fractal antenna used logarithmic spiral antenna(LFA) and Fibonacci spiral antenna (PFA) structures to generate CP with narrow ARBW which is about 1.3% of the operating band around the resonant frequency 6GHz. Other researchers reported [17–23] slot or fractal antennas with operating bands cover the requirements of Wi-Fi and WiMAX applications.

Table 1 illustrates the comparison between the proposed antenna and related antennas investigated in [4,5,6,9,10,11,12,13,14,15 and 16] about some important characteristics such : impedance bandwidth, gain, size, efficiency, ARBW and weakness points. According to **Table 1**, most of the previous related antennas are linearly polarized radiation . So, it is needed to design antenna has compact size, circularly polarized , stable radiation properties , high efficiency , and acceptable gain values that can be used for Wi-Fi and WiMAX applications.

The aim of this study is to propose a monopole meandered ring antenna that covers the frequency range of 4.5–6.5 GHz to meet specifications of the upper operating band of 5–5.9 GHz for Wi-Fi and WiMAX applications with circularly polarized radiation , high efficiency in a compact size.

Table 1. Comparison between the proposed antenna and related antennas in [3,4,5,8,9,10,11,12,13,14,15, and 16].

Ant.	BW (GHz)	Gain (dB)	Size (mm)	Efficiency %	ARBW (GHz)	Weak points
[4]	(2.3-2.7) (4.5-6)	1.9-3.9	50x10x1	55	LP	Low efficiency LP.
[5]	5.1-6.5	1.9	48x10x1.57	86	LP	Doesn't cover all bands, LP
[6]	(2.4-2.6)(5-6)	1.5-4	60x15x1.6	80	LP	Low gain at low band, LP
[9]	(5.2-5.7)	-7~ 4	30x21x0.8	-	LP	Rogers 4003 substrate, LP, covers only two bands.
[10]	(2.39–2.453)	-	30x30x1.6	-	LP	Covers only upper band , LP, no efficiency values

Ant.	BW (GHz)	Gain (dB)	Size (mm)	Efficiency %	ARBW (GHz)	Weak points
[11]	(4.5-5.6)	2-6	55 × 47 × 4.8	70-85	LP	3 conductive layers, LP and doesn't cover all required frequencies.
[12]	(1.5-4)	2.2~2.4	80x40x1.58	60-79	LP	LP, the thickness is not slandered, doesn't cover the (5-6) GHz band, complex geometry
[13]	(2.4-3.9) (4.9-5.4)	-0.5 ~2.5	45x10x0.8	-	LP	LP, doesn't cover all frequency requirements, no efficiency values
[14]	(2.4-2.49) (5.1-5.8)	1.9~7	120x120x1.6	-	LP	Large size, doesn't cover all requirement band, LP
[15]	(3.4-3.6)	6	45x40x2.5	85	0.1	Cover only 3.5GHz band, thickness too much,
[16]	(2.7-10.3)	-	54x36x1.5	85-95	1.1	No values of gain , dos not cover 2.5GHz band.
Prop.	4.5-6.5	2.2-2.4	24x9x0.8	92	0.08	Covers only upper band

3. Antenna Study

3.1 Antenna Design

In this study, the proposed antenna with a compact size of $24 \times 9 \times 0.8 \text{ mm}^3$ was configured by a three-step process. The radiator of reference antenna (**Fig. 1(a)**) is a square patch with dimensions ($X=Y=9 \text{ mm}$) and is separated from the ground by a gap g of 0.3 mm . According to the empirical equation (1), the dimension of the square patch can be calculated for the resonant frequency ($f_r = 5 \text{ GHz}$) and substrate FR-4 with $\epsilon_r = 4.3$.

$$W = \frac{c}{f_r \sqrt{\frac{\epsilon_r + 1}{2}}} = 36 \text{ mm} \quad (1)$$

To miniaturize the dimension of the antenna, let $X = Y = \frac{W}{4} = 9 \text{ mm}$

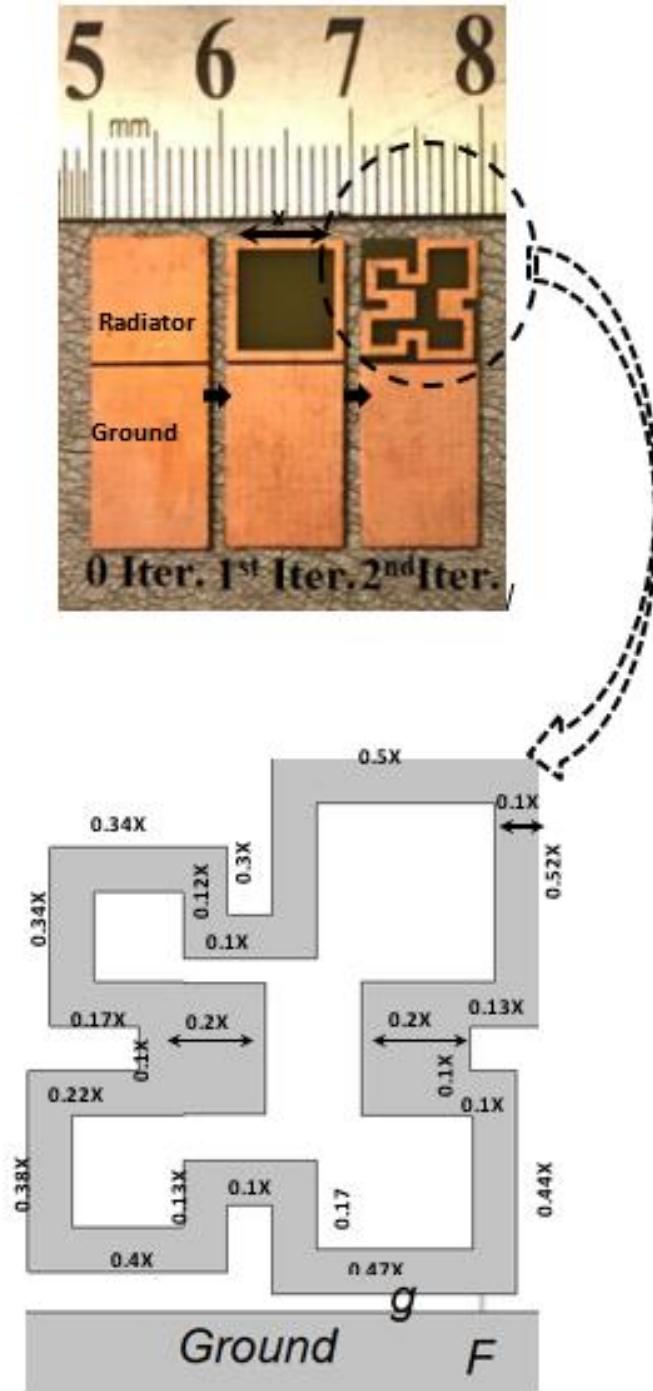


Fig. 1. The process of configuring the meandered ring antenna.

The ground plate features a rectangular shape with dimensions of $9.7 \times 9 \text{ mm}^2$. The radiator and ground are printed on the same side of the commercial substrate (FR-4) with $\epsilon_r = 4.3$, $\tan \delta = 0.027$, and thickness = 0.8 mm.

Fig. 1 (the upper part) shows the first iteration in the design of antenna with square slot cuts in the radiator plate to configure the square ring with arm width equal to $0.1X$. In the second iteration, the square ring is modified as a meandered ring to increase its electrical length to generate more resonant frequencies, which are collected to obtain a notched operating band of 4.4–6.7 GHz, as shown in **Fig. 2**. All dimensions of the meandered ring are denoted as a function of X , which corresponds to the dimension of the square ring in the first iteration, as indicated in **Fig. 1** (the lower part).

All dimensions of the meandered ring are denoted as a function of x , which corresponds to the dimension of the square ring in the first iteration, as indicated in **Fig. 1** (the lower part). The length of the square ring in the first iteration equals $(4x)$.

$$\text{Length of the upper arm} = 0.5X + 0.3x + 0.1X + 0.12X + 0.34X = 1.36X \quad (2)$$

$$\text{Length of left arm} = 0.34X + 0.17X + 0.1X + 0.22X + 0.38X = 1.21X \quad (3)$$

$$\text{Length of bottom arm} = 0.4X + 0.13X + 0.1X + 0.17X + 0.47X = 1.27X \quad (4)$$

$$\text{Length of right arm} = 0.44X + 0.1X + 0.1X + 0.13X + 0.52X = 1.29X \quad (5)$$

Thus, the total length of meandered ring equals $(5.13X)$. Length of meandered ring increases by a factor of 1.28 compared with the length of the square ring of the same size in the first iteration. Of course, the increase in length of the four arms leads to increase in the length of the surface current paths and thus generate new resonant frequencies which collected together to give a wide impedance bandwidth and this is clear in **Fig. 2** (the solid curve) where the operating band increased when the ring becomes meandered at the 2nd iteration. In **Fig. 2**, the operating band expanded during the process of meandered ring configuration.

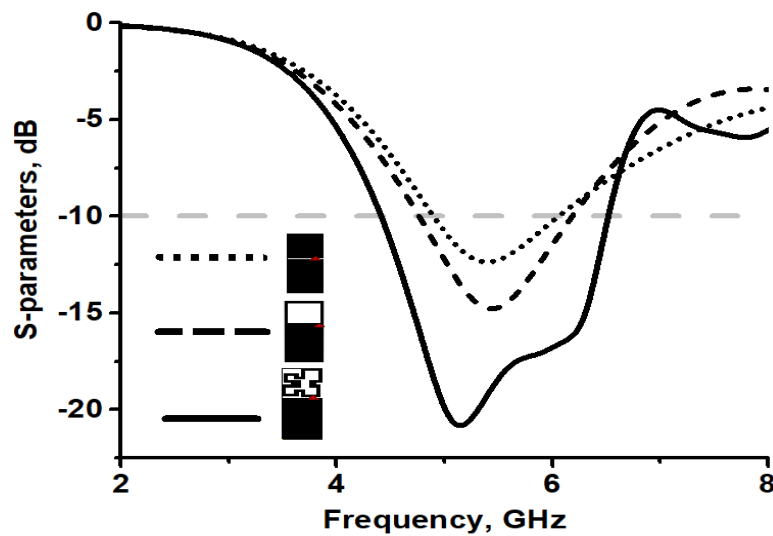


Fig. 2. The simulated reflection coefficient for the 0th iteration, 1st iteration and the 2nd iteration.

Fig. 3 depicts the real (black curves) and the imaginary (blue curves) parts of the impedance values for the three antennas. Values of real-part impedance for all antennas are almost equal at frequencies less than 4.7 GHz. Thereafter, the values of real-part impedance for the second iteration are closer to the input impedance of excitation port (50 Ohms-red line), especially at the frequency range of 5.1–6.4 GHz. **Fig. 3** shows that negative imaginary values (capacitance) are observed in curves of imaginary part impedance for all antennas at frequencies less than 4.4 GHz. At the frequency band of 4.4–6 GHz, values of imaginary part are closer to zero (red line), that is, only real-part impedances for the three antennas are almost resistant. This property gives stable matching factor which leads to stable gain and efficiency during the operating band.

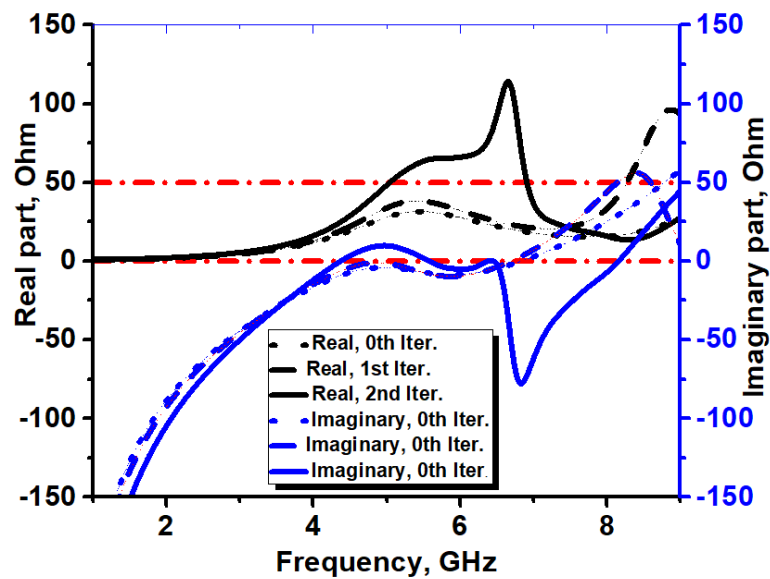


Fig. 3. The impedance values of the three iterations

Table 2 illustrates some important radiation properties for each iteration, such as, impedance bandwidth, efficiency, gain and ARBW. It's clear that most of the required specifications of antennas used for Wi-Fi and WiMAX can be achieved at the 2nd iteration due to improving the values of radiation properties during the progress of antenna configuration, especially the impedance bandwidth, efficiency, gain and an ARBW as shown in **Table 2**.

Table 2. The radiation properties for all iterations of the meandered ring fractal antenna.

Iteration	BW (5-6) (GHz)	Efficiency %	ARBW <3dB (GHz)	Gain (dB)	Lower S1,1 (dB)	State
0th	(5.2-6)	50-65	-	-12~0	-10	Low efficiency, low gain and LP.
1st	(4.7-6)	60-75	-	1~3	-14	Doesn't have stable value of gain and LP
2nd	(4.4-6.7)	85-90	0.083	2.2~2.4	-20	Optimum

3.2 Surface Current Distribution

The maximum distribution current at 5GHz for the 0iteration are mainly concentrated close to the feeding point on the patch and ground plates, as it is shown in Fig. 4 while in the 1st iteration, the currents are distributed in the additional area, especially on the square ring which leads to generate new resonant frequency than, the operating band is expanded compared with that at 0th iteration. The distribution of surface current on ground plate is the same at all iterations because there is no changed in surface current path at the ground plate during the progress of antenna configuration compared with radiator plane.

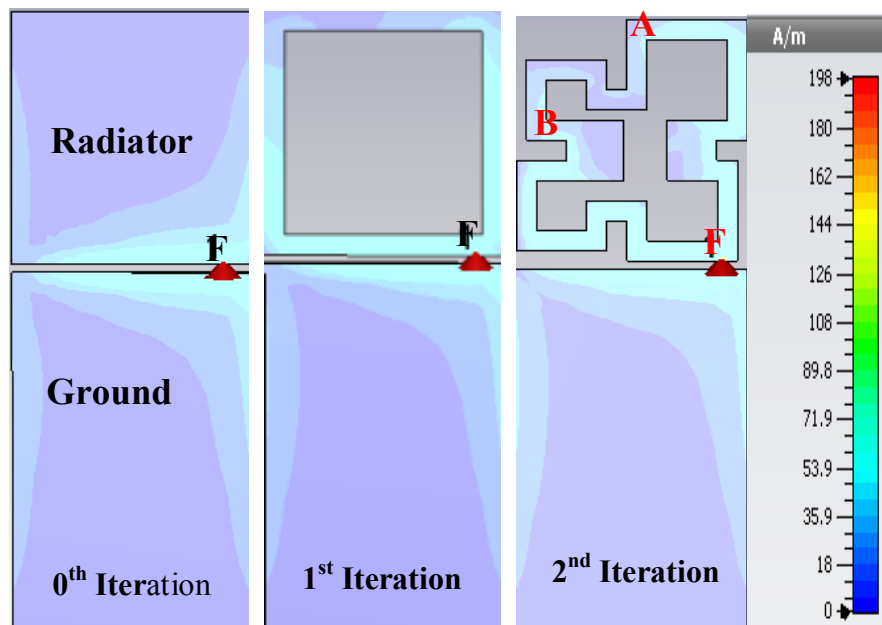


Fig. 4. The surface current at 5GHz for all iterations.

It is observed in Fig. 4 (2nd iteration) that the surface current has two paths, the first path starts from feeding point F , then passes through the right arm to the point A , it has a total length equals to $(1.79X=16\text{mm})$ which is about $\frac{1}{4}$ of the wavelength for the resonant frequency 5GHz. The other path which is almost perpendicular to the first and starts from the feeding point F then passes through the bottom arm to the point B , the total length of second path is equal to $(1.87X=17\text{mm})$ which is about $\frac{1}{4}$ of the wavelength for the resonant frequency 5GHz. So, there are two equal components of surface current normal to each other provide orthogonal components of electric fields in turn that generate circularly polarized radiation at 5GHz.

3.3 Circular Polarization

The length of the 1st surface current path from feeding point F to the point A is 16mm almost equals to the length of 2nd surface current path from feeding point to point B , these normal components are about $\frac{1}{4}$ of the wavelength for 5GHz created CP as its

clear in **Fig. 5** which represents the surface current distribution for phases 0° , 90° , 180° , and 270° at 5 GHz resonant frequency. Surface current circulates clockwise along the upper and lower right quarters and counter-clockwise along the lower left quarter for the phases 0° and 180°

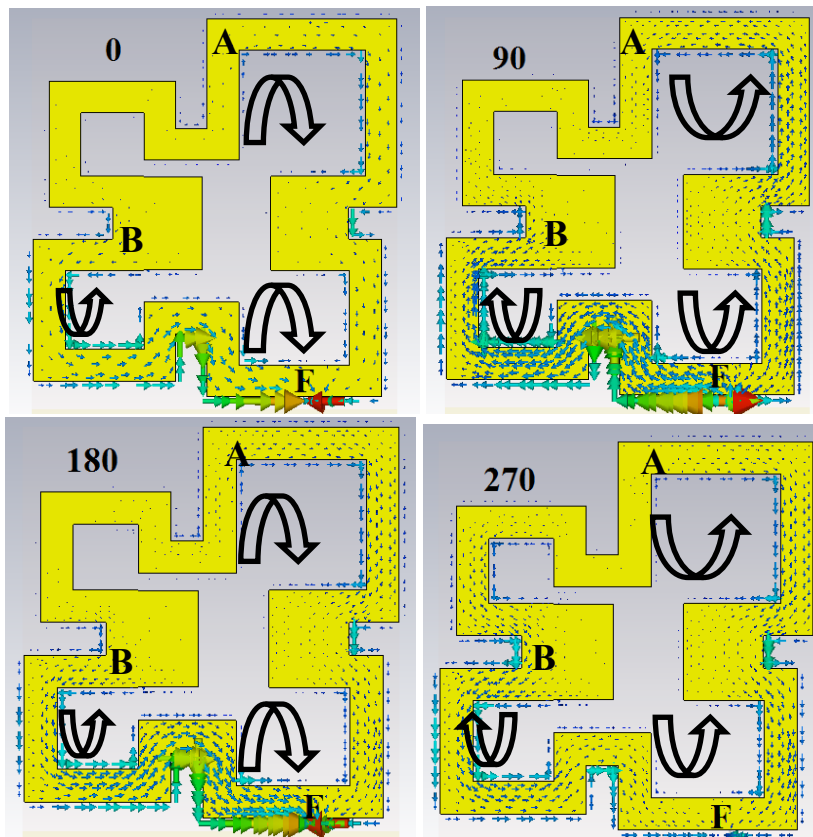


Fig. 5. Surface current for sequential phases (0° , 90° , 180° , and 270°) at 5 GHz.

Fig. 5 shows the direction of circulation the surface current when the phase becomes 90° and 270° . **Fig. 6** depicts the left and right polarizing radiation in E-plane at 5 GHz and 5.8 GHz, it's clear that the phase difference between the radiation patterns at 5 GHz is about 86 degrees while at 5.8 GHz is 180 degrees, that means, there is CP radiation at 5GHz only. This study matches the surface current distribution which indicates that there is a circular polarization radiation at 5GHz generated by dual orthogonal components of electrical field which created by surface currents that flow along the perpendicular arms of the meandered ring at the feed point as shown in **Fig. 4**.

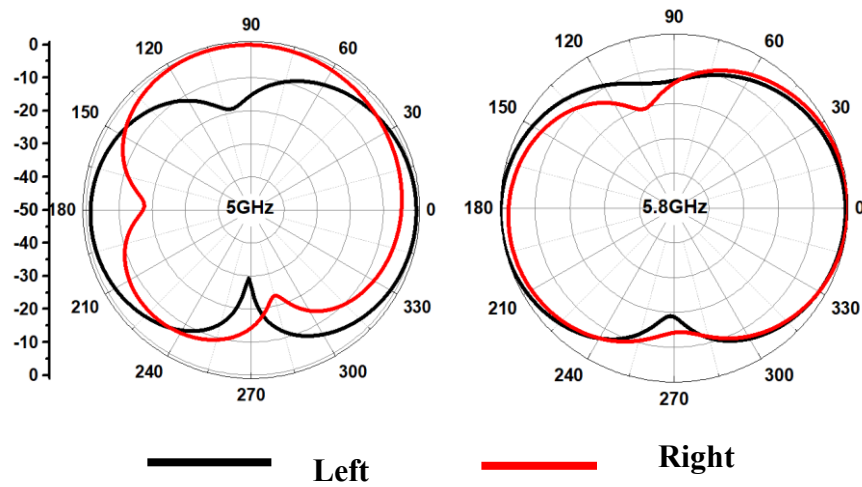


Fig. 6. Simulated left and right polarization in E-plane at 5GHz and 5.8GHz.

4. Measurements and Results

Fig. 7 represents the photographs of the all iterations prototypes, it's clear that the size of the proposed antenna is compact that can be used for portable communication devices.

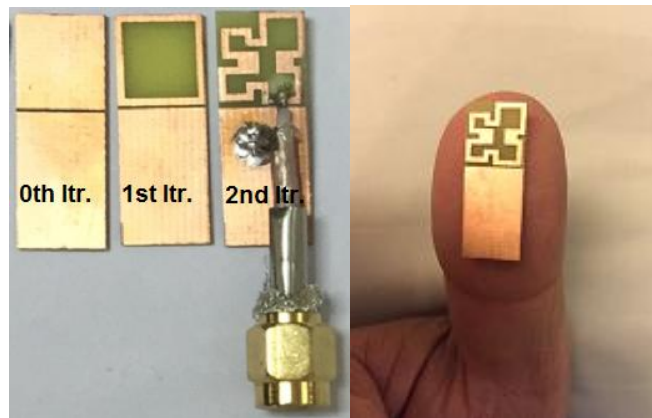


Fig. 7. The prototypes of all fractal antenna iterations.

Measured impedance bandwidth for the proposed antenna compresses to the frequency band of 4.8–6.7 GHz compared with the simulated impedance bandwidth of 4.4–6.7 GHz and the resonant frequency shifted to 5GHz compared with 5.8GHz for the simulated value as it is shown in **Fig. 8**. That takes place due to impurities of some of the materials that are used in prototypes and due to the soldering.

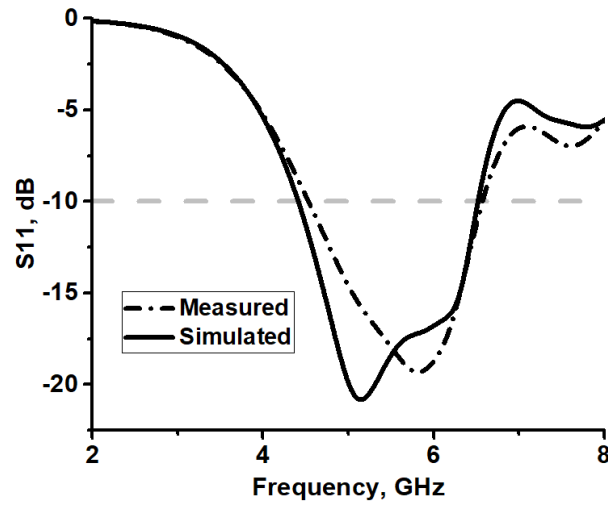


Fig. 8. The measured (dashed) and simulated (solid) $S_{1,1}$ for the proposed antenna.

Fig. 9 shows a distinguishing agreement between simulated (solid) and measured (dashed) patterns. Radiation patterns in the H-plane (black curves) for the proposed antenna are almost omnidirectional at 5 and 5.8 GHz. Figure 5.21b shows that the radiation pattern at 5.8 GHz is similar to that at 5 GHz, but the former is more directional.

At E-plane (when $\phi=0$), the radiation patterns looked like number 8 where two major lobes observed shifts by an angle of 180 degrees as its shown in **Fig. 9(a)** (the red curves) while at 5.8GHz, the radiation pattern in E-plane had dual asymmetrical major lobes.

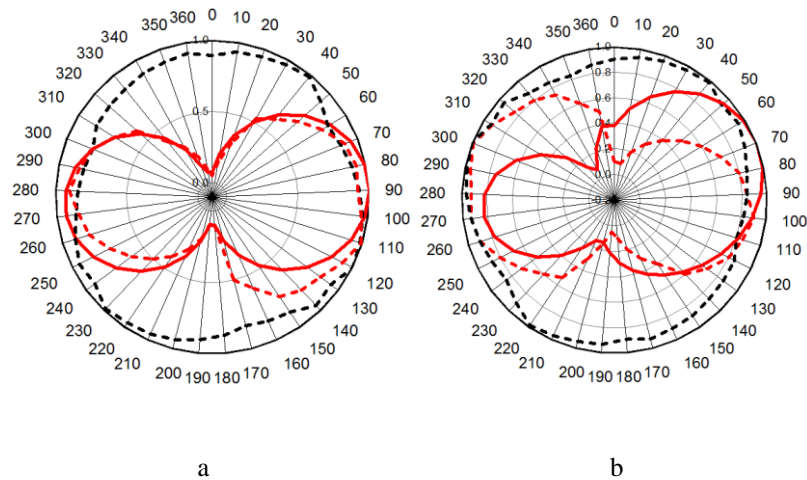


Fig. 9. Simulated (solid) and measured (dashed) radiation pattern.

- a. At 5GHz.
- b. At 5.8GHz.

Fig. 10 depicts the measured (dashed curves) and the simulated (solid curves) values of the gain, efficiency and an axial ratio. At frequency bands of 5–6 GHz, measured gain values (black dashed curve) are almost constant 2.3–2.4 dB, and measured efficiency (blue gashed curve) reaches -0.45 dB (92%), whereas measuring axial ratio bandwidth compress to the frequency range 4.95-5.2GHz (approximately 8.3% of operating band) around a resonant frequency of 5 GHz.

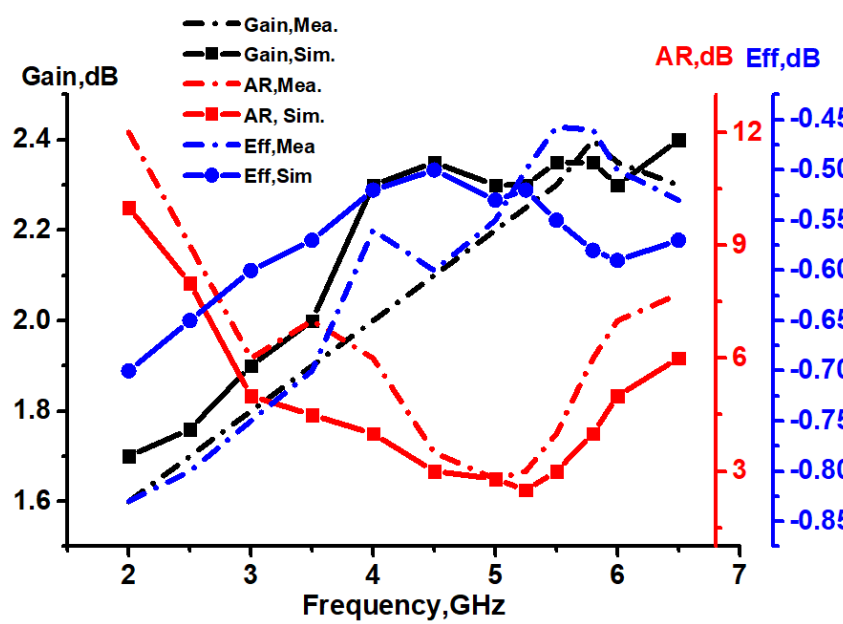


Fig. 10. Measured(dashed) and simulated (solid) gain, AR and efficiency for the antenna.

5. Conclusion

In this research, a novel fractal ring antenna presented. The proposed antenna had stable radiation properties, especially the gain and efficiency during the operating band. This feature is distinguished by the proposed antenna from the other previous antennas in addition to the compact size. Referring to **Table 1**, the proposed antenna covers only the upper bandwidth of (5GHz-5.9GHz) that is used for Wi-Fi and WiMAX applications. The proposed antenna in this study is the smallest size, low profile, higher efficiency (92%), stable gain, and a matching factor. Also, the proposed fractal ring antenna is circularly polarized with an ARBW of 83 MHz, which is about 8.3% of the operating band. Thus, the meandered ring monopole antenna compared with 11 previously related antennas is the best to be used in portable communication devices.

References

- [1] R. S. Reid, "Wi-Fi (802.11) Network Handbook," 1st Ed. ed. USA: McGraw-Hill, 2013.
- [2] S. A. M. Ilyas, "WiMAX: Standards and Security," CRC Press, 2007.
- [3] D. H. Gangul, "An overview of fractal antenna engineering research," *IEEE Antennas and Propagation Magazine*, vol. 52, no. 6, pp. 59-67, Dec 2010.

- propagation Magazine*, vol. 45 pp. 38-57, 2003., pp. 38-57, 2003., 2003.
- [4] S.J. Jeong and K.C. Hwang, "Compact loop-coupled spiral antenna for multiband wireless USB dongles," *Electron. Lett.*, 18th March 2010, 46, (6). [Article \(CrossRef Link\)](#)
 - [5] E.A. Elghannai and R.G. Rojas, "Design of USB dongle antenna for WLAN applications using theory of characteristic modes," *Electron. Lett.*, 18th March 2014, 50, (4) pp. 249–251. [Article \(CrossRef Link\)](#).
 - [6] W. Liao, S. Chang, J.T. Yeh, and B. Hsiao, "Compact Dual-Band WLAN Diversity Antennas on USB Dongle Platform," *IEEE Trans. Antennas Propag.*, vol. 26, no. 1, pp. 109–118, Jan. 2014. [Article \(CrossRef Link\)](#)
 - [7] Jui-Han Lu, Yu-Yi Lee, "Planar compact triple-band monopole antenna for IEEE 802.16 m worldwide interoperability for microwave access system," *Microwaves, Antennas & Propagation*, 2013, Vol.7, Iss. 13, pp. 1045–1054. [Article \(CrossRef Link\)](#).
 - [8] W.C. Liu and Y.-L. Chen, "Compact strip-monopole antenna for WLAN-band USB dongle application," *Electron. Lett.*, 14th April 2011 Vol. 47 No. 8. [Article \(CrossRef Link\)](#).
 - [9] T. Li, F. Huo, H. Q. Zhai, and C.H. Liang, "Compact ultra-wideband antenna with sharp band-notched characteristics for WiMax and WLAN," *Electronics letters*, vol. 48, pp. 1380-1382, 2012. [Article \(CrossRef Link\)](#)
 - [10] M. Ojaroudi, S. Bashiri, N. Ojaroudi, and M. Partovi, "Octave-band, multi-resonance CPW-fed small slot antenna for UWB applications," *Electronics letters*, vol. 48, pp. 980-982, 2012. [Article \(CrossRef Link\)](#)
 - [11] S.-O. P. Hyunseong Kang "Mushroom meta-material-based substrate integrated waveguide cavity backed slot antenna with broadband and reduced back radiation," *IET Microwaves, Antennas & Propagation*, vol. 10, pp. 1598–1603, 2016. [Article \(CrossRef Link\)](#)
 - [12] S. K. B. Yogesh Kumar Choukiker, "Wideband frequency reconfigurable Koch snowflake fractal antenna," *IET Microwaves, Antennas & Propagation*, vol. 11, 2017. [Article \(CrossRef Link\)](#)
 - [13] S. Chaimool, C. Chokchai, and P. Akkaraekthalin, "Multiband loaded fractal loop monopole antenna for USB dongle applications," *Electronics letters*, vol. 48, pp. 1446-1447, 2012. [Article \(CrossRef Link\)](#)
 - [14] W.C. Weng and C.L. Hung, "An H-Fractal Antenna for Multiband Applications," *IEEE Antennas and Wireless Propagation Letters*, vol. 13, pp. 1705-1708, 2014. [Article \(CrossRef Link\)](#)
 - [15] T. Cai, G.M. Wang, X.-F. Zhang, and J.P. Shi, "Low-profile compact circularly-polarized antenna based on fractal metasurface and fractal resonator," *IEEE Antennas and Wireless Propagation Letters*, vol. 14, pp. 1072-1076, 2015. [Article \(CrossRef Link\)](#)
 - [16] S. M. Chetna Sharma, IEEE, and Dinesh Kumar Vishwakarma, "Miniaturization of Spiral Antenna Based on Fibonacci Sequence Using Modified Koch Curve," *IEEE Antennas and Wireless Propagation Letters*, vol. 16, 2017. [Article \(CrossRef Link\)](#).
 - [17] X.L. Sun, L. Liu, S.W. Cheung, T.I. Yuk, "Dual-band antenna with compact radiator for 2.4 / 5.2 / 5.8 GHz WLAN applications," *IEEE Trans. Antennas Propag.*, 2012, 60, (12), pp. 5924–5931. [Article \(CrossRef Link\)](#)
 - [18] P. GaoShuang He, Xubo Wei, Ziqiang Xu, Ning Wang, and Yi Zheng "Compact Printed UWB Diversity Slot Antenna With 5.5-GHz Band-Notched Characteristics," *IEEE Antennas and Wireless Propagation Letters*, vol. 13, pp. 376–379, 2014. [Article \(CrossRef Link\)](#)
 - [19] W. Jiang and W. Q. Che, "A novel UWB antenna with dual notched bands for WiMAX and WLAN applications," *IEEE Antennas Wireless Propag. Lett.*, vol. 11, pp. 293–296, 2012. [Article \(CrossRef Link\)](#)
 - [20] Chow-Yen-Desmond Sim, Yuan-Kai Shih, Ming-Hsuan Chang, "Compact slot antenna for wireless local area network 2.4/5.2/5.8 GHz applications," *IET Microwaves, Antennas & Propagation*. Vol. 9, Iss. 6, pp. 495–501, 2015. [Article \(CrossRef Link\)](#)
 - [21] Jui-Han Lu and Bing-Jhang Huang, "Planar Compact Slot Antenna With Multi-Band Operation for IEEE 802.16m Application," *IEEE Trans. on Antennas Propag.*, vol. 61, no. 3, pp.1411–1414, Mar.2013. [Article \(CrossRef Link\)](#)

- [22] Amer. T. Abed, "Highly Compact Size Serpentine-Shaped MIMO Fractal Antenna with Circular Polarization Diversity," *IET Microwaves, Antennas & Propagation*. [Article \(CrossRef Link\)](#).
- [23] Amer. T. Abed, Singh, M.J., Islam, M.T, "Amer fractal slot antenna with quad operating bands high efficiency for wireless communications," *IEEE 3rd Int. Symp. on Telecommunication Technologies (ISTT)*, Kuala Lumpur, 28–30 November 2016, pp. 6–8



Amer T. Abed received Bach in Electrical Eng. from college of engineering - University of Baghdad 1984. Master in communication Eng. in 2010 from University of TENAGA Malaysia. Has wide experience in designing the RF circuit and antenna field. Many published researches in ISI journals, published a book (Backfire antenna theory and design) –Lab lambert for academic publication–Germany2013. Now a lecturer in communication engineering department, AL Mamoon University College, Baghdad-Iraq.



Mandeep Jit Singh received his B.Eng. (with honors) and Ph.D. degrees in electrical and electronic engineering from the University of Notrumbria, UK, and Universiti Sains Malaysia, in 1998 and 2006, respectively. From 2006 up to June 2009, he was attached at Universiti Sains Malaysia as a Lecturer. Currently, he is attached to the Universiti Kebangsaan Malaysia as an Associate Professor. His areas of specialization are radiowave propagation in satellite communication system, and RFID antenna design. His collaborated with the Association of Radio Industries and Business (ARIB) Japan to analyze the rain fade at Ku-band in tropical climate using satellite involving countries such as Thailand, Philippines, Indonesia, and Fiji. Current collaboration is with the National Defense Agency, Japan, Microwave Anechoic Lab Chamber and Kyutech University on antenna development. Dr. Singh has published 190 papers in ISI journals. He has reviewed more than 200 articles in impact factors journal.



Mohammad Tariqul Islam (SM'13) was born in Dhaka, Bangladesh, in 1975. He is a Professor at the Department of Electrical, Electronic and Systems Engineering of the Universiti Kebangsaan Malaysia (UKM) and visiting Professor of Kyushu Institute of Technology, Japan. He is the author of about 350 research journal articles, nearly 165 conference articles, 4 research level books and a few book chapters on various topics related to antennas, microwaves and electromagnetic radiation analysis with 12 inventory patents filed. Thus far, his publications have been cited 2700 times and his H-index is 28 (Source: Scopus). He is now handling many research projects from the Malaysian Ministry of Science, Technology and Innovation and Ministry of Education. His research interests include communication antenna design, radio astronomy antennas, satellite antennas, and electromagnetic radiation analysis.

Dr. Islam currently serves as the Editor-in-Chief for the International Journal of Electronics and Informatics and Associate Editor for International Journal of Antenna and Propagation and Electronics Letter. He received several International Gold Medal awards, a Best Invention in Telecommunication Award, a Special Award from Vietnam for his research and innovation, and Best Researcher Awards in 2010 and 2011 at UKM. He also won the best innovation award in 2011 and the Best Research Group in ICT niche in 2014 by UKM. He was the recipient of *Publication Award* from Malaysian Space Agency in 2014, 2013, 2010, 2009 and the Best Paper Presentation Award in 2012 International Symposium on Antennas and Propagation, (ISAP 2012) at Nagoya, Japan and in 2015 in Icon Space. He is a member of the Institute of Electronics, Information and Communication Engineers (IEICE) and IET.